Regional-scale jet waviness modulates the occurrence of mid-latitude weather extremes

Matthias Röthlisberger[1], Stephan Pfahl[2] and Olivia Martius[1,3]

[1]Oeschger Centre for Climate Change Research and Institute of Geography, University of Bern, Bern, Switzerland

[2]Institute for Atmospheric and Climate Science, ETH Zürich, Zürich, Switzerland

[3]Mobiliar Lab for Natural Risks, University of Bern, Bern, Switzerland

Key Points:

- Regional-scale jet waviness significantly modulates the number and location of weather extremes
- Weather extremes are primarily affected by regional-scale rather than hemispheric jet waviness
- The strength and sign of the waviness-extremes link differs between regions

Corresponding author: Matthias Röthlisberger, matthias.roethlisberger@giub.unibe.ch

Abstract

Several studies have attributed the occurrence of recent weather extremes to an amplified waviness of the upper-tropospheric jet stream. Although trends in jet waviness are still under discussion, it is crucial to better understand the mechanisms through which jet waviness affects weather extremes. Here we show that variations in jet waviness on regional scales effectively modulate the occurrence of daily weather extremes, however, in regionally different ways. The jet waviness over the North Atlantic and the North Pacific mainly affects where wind, precipitation and cold extremes occur, while a wavy jet over Eurasia strongly favors the occurrence of hot extremes in summer. This is because regional variations of jet waviness are intrinsically linked to the occurrence and tracks of synoptic-scale weather systems, which can trigger the extremes. We conclude that potential jet waviness changes would affect the occurrence of weather extremes differently depending on where these changes occur.

1 Introduction

In recent years the Northern Hemisphere mid-latitudes have been hit by a remarkable series of high-impact weather extremes including the record breaking heat waves in Europe in 2003 [*Black et al.*, 2004] and in Russia in 2010 [*Barriopedro et al.*, 2011], severe floods in the United Kingdom in 2013/2014 [*Herring et al.*, 2014] and unusually cold winters with devastating winter storms in the eastern United States [*Palmer*, 2014; *Vose et al.*, 2014]. The number, diversity and severity of these weather extremes has triggered an engaged debate on the causes of their temporally clustered occurrence. While a change in the frequency of some extremes is expected with global warming [*IPCC*, 2012; *Coumou and Rahmstorf*, 2012; *Schneider et al.*, 2015; *Hoskins and Woollings*, 2015], most studies agree that the recent series of mid-latitude weather extremes cannot be explained by the observed shift in the mean temperature and thermodynamic arguments alone [*Horton et al.*, 2015]. Hence, these weather extremes must at least partly be related to anomalous atmospheric circulation patterns [*Horton et al.*, 2015; *Hoskins and Woollings*, 2015].

Several studies have proposed that increased waviness of the polar jet has favored the occurrence of particular weather extremes [*Francis and Vavrus*, 2012; *Petoukhov et al.*, 2013; *Screen and Simmonds*, 2014; *Francis and Vavrus*, 2015; *Francis and Skific*, 2015]. Previous studies investigating this "waviness-extremes" link have mainly focused on long-lasting extremes on continental to hemispheric scales [*Liu et al.*, 2012; *Petoukhov et al.*, 2013; *Coumou et al.*, 2014; *Screen and Simmonds*, 2014]. Statistically significant links between jet waviness on a

hemispheric scale and monthly temperature and precipitation extremes could be established for several mid-latitude regions [*Screen and Simmonds*, 2014]. On synoptic (multi-day) timescales, periods of frequently occurring temperature and precipitation extremes have recently been linked to low- and high storm track activity, respectively [*Lehmann and Coumou*, 2015; *Coumou et al.*, 2015]. However, one particularly important aspect of this topic has not been investigate so far, namely regional variations in the strength and sign of this link.

A variety of jet waviness measures have been proposed in recent studies. Some of them conceptualize jet waviness as the amplitudes of the excursions of geopotential height isopleths or isentropic PV contours from a zonal background state [*Francis and Vavrus*, 2012, 2015; *Screen and Simmonds*, 2013a; *Röthlisberger et al.*, 2016]. Others rely on Fourier analysis of the meridional wind or the geopotential height in particular latitude bands [*Petoukhov et al.*, 2013; *Coumou et al.*, 2014; *Screen and Simmonds*, 2013a, 2014] as an indication for wave amplitudes. The use of these conceptually different types of waviness measures may lead to contradicting results, as a number of studies has shown that trends in jet waviness as inferred from these different measures do not generally agree [*Barnes*, 2013; *Barnes and Screen*, 2015; *Screen and Simmonds*, 2013b].

Here, we use the regional-scale jet waviness measure introduced by *Röthlisberger et al.* [2016] only to discriminate between regionally wavy and zonal upper-level flow configurations and investigate, where and how a regionally wavy (or zonal) jet favors or hampers the occurrence of daily weather extremes.

It is well established that mid-latitude weather extremes often occur in association with synoptic-scale weather systems such as cyclones and blocking anticyclones and that these weather systems are steered by the upper-level flow [e.g., *Dickson and Namias*, 1976; *Davies*, 2015]. For example precipitation and wind extremes in winter occur preferentially in or near extratropical cyclones [*Donat et al.*, 2010; *Pfahl and Wernli*, 2012a; *Vose et al.*, 2014]. Winter cold extremes in western Europe and the Mediterranean often occur during cold air outbreaks downstream of North Atlantic blocking [*Sillmann et al.*, 2011; *Buehler et al.*, 2011] and in the same way blocking over the North Pacific favors cold extremes in western North America [*Whan et al.*, 2016]. Summer heat extremes, in contrast, tend to occur near the center of blocking anticyclones [*Pfahl and Wernli*, 2012b], mainly for two reasons: Firstly, subsiding air within the blocks and the resulting clear sky conditions lead to increased solar irradiation reaching the Earth's surface [*Black et al.*, 2004; *Barriopedro et al.*, 2011; *Pfahl and Wernli*, 2012b]. Sec-

ondly, the adiabatic warming of the subsiding air leads to reduced relative humidity and prevents precipitation. The lack of precipitation as well as the increased solar irradiation both contribute to soil moisture depletion which in turn increases the surface sensible heat flux [e.g., *Namias*, 1960; *Fischer et al.*, 2007; *Seneviratne et al.*, 2010]. Over the oceans the influence of blocking on extreme temperature is much reduced, on the one hand due to the larger heat capacity compared to the land surface (and hence less temperature variability on synoptic time scales) but also due to the lack of the soil-moisture coupling [*Pfahl and Wernli*, 2012b].

From a meteorological point of view it is therefore clear that weather systems are crucial for understanding the waviness-extremes link. However, in the recent literature their pivotal role in linking the upper-level flow to surface weather extremes has not been considered sufficiently. In this study we thus aim to contribute to this current discussion in two ways: Firstly, we analyze this waviness-extremes link regionally and show that the strength and sign of this link varies between regions and types of extremes. Secondly, we use feature based climatologies of extratropical cyclones and blocking anticyclones to illustrate the regionally varying role of weather systems in linking jet waviness to the occurrence of surface weather extremes.

2 Data and Methods

2.1 Extremes and Jet Waviness Data

The ERA-Interim re-analysis data set [*Dee et al.*, 2011] (interpolated to $1\,^\circ \times 1\,^\circ$ horizontal resolution, covering the period of 1979-2012) is used to identify daily extremes of daily maximum 10 m wind gusts (ERA-Interim variable "10 metre wind gust since previous post-processing"), daily maximum 2 m temperature, daily minimum 2 m temperature and daily accumulated precipitation as the 5% most extreme values per season at every grid point. These data stem from short term model predictions (with lead times between 6 and 18 h) of the European Centre for Medium-Range Weather Forecasts (ECMWF) Integrated Forecast System (IFS) model which was used for producing the ERA-Interim data set. Note that the absolute values of the extremes are largely irrelevant for our analysis. Rather it is the timing of the extreme events that matters for this analysis and previous studies have reported that in the extratropics this timing is reasonably well represented in ERA-Interim [*Pfahl and Wernli*, 2012a].

The waviness of the polar jet is measured separately in the Eurasian (0 °E-135 °E), North Pacific (135 °E-120 °W), North American (120 °W-60 °W) and North Atlantic (60 °W-0 °E) sectors using the jet waviness measure introduced by *Röthlisberger et al.* [2016]. This wavi-

ness measure is based on isentropic potential vorticity (PV) fields from ERA-Interim (on the 320 K isentrope in winter and on 335 K in summer), and uses the geometry of the 2 potential vorticity unit (PVU) contours on these isentropes as an indicator for the waviness of the polar jet. The 2 PVU contour (i.e., the dynamical tropopause) on these isentropes is co-located with the polar jet and hence the contour geometry is an excellent indicator for the waviness of the polar jet. The jet waviness of a particular longitudinal sector is calculated by integrating absolute values of latitude changes of the 2 PVU contour along this contour over the length of the sector. High waviness results from large-amplitude meridional meanders of the polar jet, while low waviness is obtained for zonally orientated jet segments. The waviness values are calculated from 6-hourly PV fields and then averaged to obtain daily waviness time series covering the period 1979-2012 for all sectors. High (low) waviness days for a particular sector are defined as days on which the respective waviness value falls into the highest (lowest) quartile of the waviness distribution of the respective season and sector. The technical details of the waviness measure are described in Supporting Text S1 [*Martius et al.*, 2010].

2.2 Odds Ratios

Using these extremes and jet waviness data, the odds ratio (OR) of the occurrence of an extreme during high (low) waviness in a particular sector is calculated at each grid point as

$$\mathrm{OR} = \frac{P(Ext|Wave)(1-P(Ext))}{P(Ext)(1-P(Ext|Wave))} \tag{1}$$

where $P(Ext|Wave)$ is the probability of observing an extreme at the respective grid point during a day with high (low) waviness, estimated as the number of high (low) waviness days with a co-occurring extreme divided by the total number of high (low) waviness days. $P(Ext)$ is the probability of observing an extreme at any day, i.e., 0.05. With this approach we thus assess, how frequently weather extremes co-occur with a regionally wavy (or zonal) jet compared to their climatological frequency (see *Stephenson* [2000] and Chapter 8.2.2 in *Wilks* [2011] for a discussion of the use of odds ratios in atmospheric sciences).

The significance of the ORs is assessed in a two step approach. First, a Monte-Carlo method is applied to estimate p-values of the ORs at each grid point. Random waviness time series are constructed for each region and season by shuffling the 34 seasons of the original time series and connecting these shuffled seasons to a random 34-season waviness time series. This

shuffling of entire seasons is necessary, as for some sectors, the original waviness time series exhibit substantial sub-seasonal variability, which, if not taken into account, strongly affects the resulting p-values. By shuffling entire seasons, however, we ensure that the random time series retain the autocorrelation and sub-seasonal variability of the original waviness data. This procedure is repeated 1000 times, and p-values at each grid point are estimated through comparison with the distribution of ORs from these samples. In a second step, the False Discovery Rate (FDR) test by *Benjamini and Hochberg* [1995] is applied to the entire set of p-values from a given OR field. This test controls the number of falsely rejected null hypotheses in multiple statistical testing. A maximum false discovery rate of 5% is chosen here. Note that, while this test was originally developed for independent data, *Ventura et al.* [2004] have shown that it also correctly controls the number of falsely rejected hypotheses in applications with spatially correlated climatological data.

2.3 Blocking and Extratropical Cyclone Climatologies

To interpret the OR fields we incorporate objective climatologies of atmospheric blocking and extratropical cyclones into our analysis. We use the algorithm developed by *Schwierz et al.* [2004] to compile a climatology of atmospheric blocking and an updated version of the cyclone climatology of *Wernli and Schwierz* [2006] (see Supporting Texts S2 and S3 for descriptions of the identification algorithms). The seasonal climatologies of atmospheric blocking and extratropical cyclones are shown in Supporting Figure 1.

3 Results and Discussion

3.1 Spatially Aggregated Effect of Regional-Scale and Hemispheric Jet Waviness on Weather Extremes

We first discuss the effect of linking regional-scale rather than hemispheric jet waviness with the extremes. Previous studies found that prolonged weather extremes, especially over land areas, occur more frequently during periods with high jet waviness on a hemispheric scale [*Liu et al.*, 2012; *Petoukhov et al.*, 2013; *Coumou et al.*, 2014; *Screen and Simmonds*, 2014]. Here we investigate, whether high regional-scale jet waviness is also consistently linked to more extremes. Figure 1 depicts the size of the northern hemisphere land area with significant ORs for high waviness and all four types of extremes. For high waviness, the majority of the significant ORs is larger than one, while the opposite is true for low jet waviness (Supporting Fig-

ure 2). Thus, there is a general tendency for more daily wind, precipitation, cold and hot extremes when the jet is regionally wavy. Locally, though, the opposite may be the case; for example the odds of winter cold extremes over western Canada and Alaska are decreased when the jet is wavy in the North American sector (see Figures 1 and 3, Supporting Figure 3 and discussion in Section 3.3).

Carrying out the same analysis for hemispheric jet waviness shows that for both high and low waviness, the land area of significant ORs is smaller for hemispheric than regional-scale jet waviness (Figure 1, Supporting Figure 2). Hence, daily weather extremes are affected primarily by regional-scale rather than hemispheric jet waviness. We next study the link between regional-scale jet waviness and extremes in more detail to show why the link is stronger on regional scales and which flow configurations and synoptic weather patterns contribute to the extremes.

3.2 Precipitation and Wind Extremes

We start with the ORs of winter (December-February, DJF) precipitation and wind extremes for high waviness in the North Atlantic sector (Figure 2(a,b)). A wavy North Atlantic jet is associated with more frequent precipitation and wind extremes over northeastern Canada, Greenland and off the coast of Morocco (odds increased by 50-150%), while over the British Isles and parts of western Europe precipitation and wind extremes are less frequent (odds reduced by up to 75%). Moreover, a wavy North Atlantic jet is associated with more cyclones between Newfoundland and Greenland and off the coast of Morocco, as well as a reduced cyclone frequency in the northeastern North Atlantic (Figure 2(a,b)).

The modulation of the cyclone frequencies explains the spatial patterns of the wind and precipitation extreme ORs: as expected from prior knowledge, wind and precipitation extremes are more frequent in areas with more cyclones. This is further illustrated for two grid points located in the areas of high OR over the Davis Strait at 57 °W/62 °N and over the eastern subtropical Atlantic at 15 °W/32 °N (Figure 2(c,d)). Precipitation extremes over the Davis Strait during winter are associated with a cyclonically overturning dynamical tropopause, i.e. cyclonic Rossby wave breaking, over the western North Atlantic, which produces the high waviness signal (Figure 2(c)). More frequent extratropical cyclones over Baffin Island and very high amounts of moisture favor the occurrence of precipitation extremes (Figure 2(c)). The synoptic situation for wind extremes over the Davis Strait is similar (Supporting Figure S4). Precipitation

extremes over the subtropical eastern Atlantic occur during anticyclonic Rossby wave breaking events over the subtropical Atlantic (Figure 2(d)) and are associated with an enhanced cyclone frequency as well as increased atmospheric moisture content in the area of the precipitation extremes. These two composites illustrate a pivotal difficulty that arises when studying the link between jet waviness and weather extremes: The high waviness days contain several distinct synoptic flow configurations, even for relatively small longitudinal sectors, and extremes in different areas of significant ORs do not necessarily occur on the same day. The statistical analyses only pick up the most dominant of these flow configurations. Considering hemispheric waviness thus leads to a strong "smoothing" of the synoptic link to the extremes and hence less statistically significant ORs.

Results for other sectors and seasons further emphasize the key role of weather systems in linking jet waviness to precipitation and wind extremes. For North Pacific jet waviness, OR patterns are qualitatively similar to those for the North Atlantic (Supporting Figure 5). For high Eurasian jet waviness significant ORs of wind and precipitation extremes are confined to the Asian high Arctic (Supporting Figure 6), where these extremes are favored by high jet waviness. In regions where extratropical cyclones occur less frequently (Supporting Figure 1) ORs of wind and precipitation extremes for high Eurasian jet waviness are similar to climatology (Supporting Figure 6). During the summer months (July-August, JJA) OR patterns for wind and precipitation extremes are qualitatively similar to winter (Supporting Figure 7), however, the signals are weaker, conceivably due to the reduced number and intensity of extratropical cyclones [*Wernli and Schwierz*, 2006] and more extremes occurring in association with smaller scale processes such as convection.

3.3 Cold Extremes

We next look at cold extremes during DJF in the Atlantic sector (Figure 3(a)). A wavy North Atlantic jet is associated with more frequent blocking situations over the central North Atlantic and an increased number of cold extremes downstream in western Europe and parts of the Mediterranean (Figure 3(a)). During days when cold extremes in western France at 4 °W/48 °N co-occur with high North Atlantic waviness, the blocking frequency is increased over the North Atlantic and easterly and northeasterly winds advect cold air to western Europe (i.e., to the south and downstream of the blocks, Figure 3(d)). This is in good agreement with previous results of *Sillmann et al.* [2011] and *Buehler et al.* [2011]. There is also an area of significant ORs in the subtropical Atlantic. Cold extremes in this region are related to an anticyclonic over-

turning of the tropopause over the subtropical Atlantic with a trough reaching far southward bringing the cold air into the subtropics (Figure 3(c)). This flow configuration is accompanied by an anomalously high blocking frequency upstream and to the north, over the western Atlantic. Again cold extremes over the subtropical Atlantic and western Europe are linked to distinctly different, but all high waviness, upper-level flow configurations over the Atlantic.

Furthermore, a wavy jet over North America is associated with less frequent cold extremes over vast areas of western Canada and Alaska, as well as more frequent blocking over central Canada (Figure 3(b)). Hence, these reduced odds conceivably result from more frequent warm air advection and suppressed cold air advection in the western part of the blocks (see also Supporting Figure 3).

3.4 Hot Extremes

Recent studies have suggested that changes in summer circulation might contribute significantly to a further increase in the number of hot extremes [*Francis and Vavrus*, 2012, 2015; *Horton et al.*, 2015; *Coumou et al.*, 2015], the hypothesis being that a more wavy jet stream is associated with more frequent atmospheric blocks [*Francis and Vavrus*, 2012; *Liu et al.*, 2012; *Francis and Vavrus*, 2015], which are conducive to summer hot extremes [*Black et al.*, 2004; *Barriopedro et al.*, 2011; *Pfahl and Wernli*, 2012b; *Horton et al.*, 2015].

Indeed, a regionally wavy jet over the Northern Hemisphere land masses favors the occurrence of hot extremes (Figure 4). Over western Russia, for example, in the region where the Russian heat wave in 2010 was most pronounced [*Barriopedro et al.*, 2011], the odds of summer hot extremes are increased by up to 150% during days with a wavy Eurasian jet (Figure 4(a)). In the same area, the frequency of atmospheric blocking is increased by roughly 50% compared to climatology (Figure 4(a) and Supporting Figure 1). A similar link is evident over eastern Siberia and over North America, (Figure 4(a) and (b)), where a wavy jet in summer favors more atmospheric blocking over Canada and is associated with more frequent hot extremes south of the Baffin Bay. Over the oceans, however, the ORs of summer hot extremes do not differ significantly from climatology during days with high regional-scale jet waviness (Supporting Figure 8), which is consistent with the findings of *Pfahl and Wernli* [2012b], as discussed in Section 1.

4 Summary and Conclusions

This study reveals a statistically highly significant and meteorologically explicable link between regional-scale jet waviness and the occurrence of different types of daily mid-latitude weather extremes. Regional-scale jet waviness affects daily weather extremes through its linkage to synoptic-scale weather systems (cyclones and blocking) that trigger the extremes. In winter, the link between jet waviness and the occurrence of daily wind, precipitation and cold extremes is strongest in and around the Northern Hemisphere storm tracks, where these extremes occur mostly in association with synoptic-scale weather systems. Further away from the storm tracks, the odds of daily wind, precipitation and cold extremes are not significantly affected by regional-scale jet waviness. In summer, the waviness-extremes linkage weakens for wind and precipitation extremes, however, high jet waviness over the continents strongly enhances the number of hot extremes by favoring the occurrence of atmospheric blocking.

While the presented results are consistent with previous findings on the role of weather systems in triggering extremes, they also clearly show that the strength and sign of the waviness-extremes link varies depending on sector, season and type of extreme. This implies that if jet waviness is to change in regionally differing ways [*Francis and Vavrus*, 2012; *Screen and Simmonds*, 2013a; *Francis and Vavrus*, 2015; *Francis and Skific*, 2015], the implications for the occurrence of extremes will fundamentally depend on where jet waviness changes occur.

Compared to previous studies that investigated the linkage of weather extremes to hemispheric jet waviness [*Liu et al.*, 2012; *Petoukhov et al.*, 2013; *Coumou et al.*, 2014; *Screen and Simmonds*, 2014], the regional-scale waviness measure used here, enables clearer and more significant associations with weather extremes. In addition, the meteorological mechanisms responsible for this linkage are shown by incorporating changes in the frequency of synoptic-scale weather systems. Our findings have the following important implications for the discussion of altered weather extremes due to changes in jet waviness.

1. The link between jet waviness and the occurrence of weather extremes is stronger for regional-scale than hemispheric jet waviness and also varies between regions. Hence, waviness changes on regional scales are more relevant for changes in the frequency of weather extremes than changes in hemispheric jet waviness. Therefore, potential changes in jet waviness need to be identified regionally.
2. Jet waviness is linked to the occurrence of daily weather extremes via synoptic-scale weather systems. To understand future changes in the occurrence of daily weather ex-

tremes in the mid-latitudes, future research needs to assess how climate change affects the number, intensity and pathway of synoptic-scale weather systems as well as their ability to trigger extremes.

Acknowledgments

The authors thank the ECMWF for providing access to the ERA-Interim data, R. Beerli (ETH Zürich) for helpful discussions about hypothesis testing and two reviewers which helped greatly to improve the clarity of this manuscript. M.R. wishes to acknowledge the Swiss National Science foundation for its financial support (Grant number $200021\_159905/1$). ERA-Interim data can be accessed under http://apps.ecmwf.int/datasets/data/interim-full-daily.

References

Barnes, E. A. (2013), Revisiting the evidence linking Arctic amplification to extreme weather in midlatitudes, *Geophys. Res. Lett.*, *40*, 4734–4739, doi:10.1002/grl.50880.

Barnes, E. A., and J. A. Screen (2015), The impact of Arctic warming on the midlatitude jet-stream: Can it? Has it? Will it?, *Wiley Interdiscip. Rev. Clim. Chang.*, *6*, 277–286, doi:10.1002/wcc.337.

Barriopedro, D., E. M. Fischer, J. Luterbacher, R. M. Trigo, and R. García-Herrera (2011), The hot summer of 2010: redrawing the temperature record map of Europe, *Science*, *332*, 220–224, doi:10.1126/science.1201224.

Benjamini, Y., and Y. Hochberg (1995), Controlling the false discovery rate: a practical and powerful approach to multiple testing, *J. Roy. Stat. Soc. B Met.*, *57*, 289–300.

Black, E., M. Blackburn, G. Harrison, B. Hoskins, and J. Methven (2004), Factors contributing to the summer 2003 European heatwave, *Weather*, *59*, 217–223, doi:10.1256/wea.74.04.

Buehler, T., C. C. Raible, and T. F. Stocker (2011), The relationship of winter season North Atlantic blocking frequencies to extreme cold or dry spells in the ERA-40, *Tellus A*, *63*, 212–222, doi:10.1111/j.1600-0870.2010.00492.x.

Coumou, D., and S. Rahmstorf (2012), A decade of weather extremes, *Nat. Clim. Change*, *2*, 491–496, doi:10.1038/nclimate1452.

Coumou, D., V. Petoukhov, S. Rahmstorf, S. Petri, and H. J. Schellnhuber (2014), Quasi-resonant circulation regimes and hemispheric synchronization of extreme weather in boreal summer, *P. Natl. Acad. Sci. USA*, *111*, 12,331–12,336, doi:

10.1073/pnas.1412797111.

Coumou, D., J. Lehmann, and J. Beckmann (2015), The weakening summer circulation in the Northern Hemisphere mid-latitudes, *Science*, *348*, 324–327, doi: 10.1126/science.1261768.

Davies, H. C. (2015), Weather chains during the 2013/2014 winter and their significance for seasonal prediction, *Nat. Geosci.*, *8*, 833837, doi:10.1038/ngeo2561.

Dee, D. P., S. M. Uppala, A. J. Simmons, P. Berrisford, P. Poli, S. Kobayashi, U. Andrae, M. A. Balmaseda, G. Balsamo, P. Bauer, P. Bechtold, A. C. M. Beljaars, L. van de Berg, J. Bidlot, N. Bormann, C. Delsol, R. Dragani, M. Fuentes, A. J. Geer, L. Haimberger, S. B. Healy, H. Hersbach, E. V. Hólm, L. Isaksen, P. Kallberg, M. Köhler, M. Matricardi, A. P. McNally, B. M. Monge-Sanz, J. J. Morcrette, B. K. Park, C. Peubey, P. de Rosnay, C. Tavolato, J. N. Thépaut, and F. Vitart (2011), The ERA-Interim reanalysis: Configuration and performance of the data assimilation system, *Q. J. Roy. Meteor. Soc.*, *137*, 553–597, doi:10.1002/qj.828.

Dickson, R. R., and J. Namias (1976), North American influences on the circulation and climate of the North Atlantic sector, *Mon. Weather Rev.*, *104*(10), 1255–1265, doi: 10.1175/1520-0493(1976)104¡1255:NAIOTC¿2.0.CO;2.

Donat, M. G., G. C. Leckebusch, J. G. Pinto, and U. Ulbrich (2010), Examination of wind storms over Central Europe with respect to circulation weather types and NAO phases, *Int. J. Climatol.*, *30*(9), 1289–1300, doi:10.1002/joc.1982.

Fischer, E. M., S. Seneviratne, P. Vidale, D. Lüthi, and C. Schär (2007), Soil moisture-atmosphere interactions during the 2003 European summer heat wave, *J. Climate*, *20*(20), 5081–5099, doi:10.1175/JCLI4288.1.

Francis, J., and N. Skific (2015), Evidence linking rapid Arctic warming to mid-latitude weather patterns, *Phil. Trans. R. Soc. A*, *373*, 20140,170, doi:0.1098/rsta.2014.0170.

Francis, J. A., and S. J. Vavrus (2012), Evidence linking Arctic amplification to extreme weather in mid-latitudes, *Geophys. Res. Lett.*, *39*(6), doi:10.1029/2012GL051000.

Francis, J. A., and S. J. Vavrus (2015), Evidence for a wavier jet stream in response to rapid Arctic warming, *Environ. Res. Lett.*, *10*(1), doi:10.1088/1748-9326/10/1/014005.

Herring, S. C., M. P. Hoerling, T. C. Peterson, and P. A. Stott (2014), Explaining extreme events of 2013 from a climate perspective, *Bull. Amer. Meteorol. Soc.*, *95*, S1–S104, doi:10.1175/1520-0477-95.9.S1.1.

354 Horton, D. E., N. C. Johnson, D. Singh, D. L. Swain, B. Rajaratnam, and N. S. Diffen-
355 baugh (2015), Contribution of changes in atmospheric circulation patterns to extreme
356 temperature trends, *Nature*, *522*, 465–469, doi:10.1038/nature14550.

357 Hoskins, B. J., and T. Woollings (2015), Persistent extratropical regimes and climate ex-
358 tremes, *Current Climate Change Reports*, *1*, 115–124, doi:10.1007/s40641-015-0020-8.

359 IPCC (2012), *Managing the Risks of Extreme Events and Disasters to Advance Climate*
360 *Change Adaptation. A Special Report of Working Groups I and II of the Intergovernmental*
361 *Panel on Climate Change*, 582 pp., Cambridge University Press.

362 Lehmann, J., and D. Coumou (2015), The influence of mid-latitude storm tracks on hot,
363 cold, dry and wet extremes, *Sci. Rep.*, *5*(17491), doi:10.1038/srep17491.

364 Liu, J., J. A. Curry, H. Wang, M. Song, and R. M. Horton (2012), Impact of declining
365 Arctic sea ice on winter snowfall, *Proc. Natl. Acad. Sci. USA*, *109*, 4074–4079, doi:
366 10.1073/pnas.1114910109.

367 Martius, O., C. Schwierz, and H. C. Davies (2010), Tropopause-level waveguides, *J.*
368 *Atmos. Sci.*, *67*, 866–879, doi:10.1175/2009JAS2995.1.

369 Namias, J. (1960), Factors in the initiation, perpetuation and termination of drought, *Inter-*
370 *national Association of Scientific Hydrology Commission on Surface Waters Publication*,
371 *51*, 81–94.

372 Palmer, T. (2014), Record-breaking winters and global climate change, *Science*, *344*,
373 803–804, doi:10.1126/science.1255147.

374 Petoukhov, V., S. Rahmstorf, S. Petri, and H. J. Schellnhuber (2013), Quasiresonant ampli-
375 fication of planetary waves and recent Northern Hemisphere weather extremes, *P. Natl.*
376 *Acad. Sci. USA*, *110*, 5336–5341, doi:10.1073/pnas.1222000110.

377 Pfahl, S., and H. Wernli (2012a), Quantifying the relevance of cyclones for precipitation
378 extremes, *J. Climate*, *25*, 6770–6780, doi:10.1175/JCLI-D-11-00705.1.

379 Pfahl, S., and H. Wernli (2012b), Quantifying the relevance of atmospheric blocking
380 for co-located temperature extremes in the Northern Hemisphere on (sub-) daily time
381 scales, *Geophys. Res. Lett.*, *39*(12), doi:10.1029/2012GL052261.

382 Röthlisberger, M., O. Martius, and H. Wernli (2016), An algorithm for identifying the
383 initiation of synoptic-scale Rossby waves on potential vorticity waveguides, *Q. J. Roy.*
384 *Meteor. Soc.*, *142*(695), 889–900, doi:10.1002/qj.2690.

385 Schneider, T., T. Bischoff, and H. Płotka (2015), Physics of changes in synoptic mid-
386 latitude temperature variability, *J. Climate*, *28*, 2312–2331, doi:10.1175/JCLI-D-14-

387 00632.1.

388 Schwierz, C., M. Croci-Maspoli, and H. Davies (2004), Perspicacious indicators of atmo-
389 spheric blocking, *Geophys. Res. Lett.*, *31*(6), doi:10.1029/2003GL019341.

390 Screen, J. A., and I. Simmonds (2013a), Exploring links between Arctic amplification and
391 mid-latitude weather, *Geophys. Res. Lett.*, *40*, 959–964, doi:10.1002/grl.50174.

392 Screen, J. A., and I. Simmonds (2013b), Caution needed when linking weather extremes
393 to amplified planetary waves, *Proceedings of the National Academy of Sciences*, *110*(26),
394 E2327–E2327, doi:10.1073/pnas.1304867110.

395 Screen, J. A., and I. Simmonds (2014), Amplified mid-latitude planetary waves
396 favour particular regional weather extremes, *Nat. Clim. Change*, *4*, 704–709, doi:
397 10.1038/nclimate2271.

398 Seneviratne, S. I., T. Corti, E. L. Davin, M. Hirschi, E. B. Jaeger, I. Lehner, B. Or-
399 lowsky, and A. J. Teuling (2010), Investigating soil moisture–climate interactions
400 in a changing climate: A review, *Earth-Science Reviews*, *99*(3), 125–161, doi:
401 10.1016/j.earscirev.2010.02.004.

402 Sillmann, J., M. Croci-Maspoli, M. Kallache, and R. W. Katz (2011), Extreme cold winter
403 temperatures in Europe under the influence of North Atlantic atmospheric blocking, *J.*
404 *Climate*, *24*, 5899–5913, doi:10.1175/2011JCLI4075.1.

405 Stephenson, D. B. (2000), Use of the odds ratio for diagnosing forecast skill, *Weather*
406 *Forecast.*, *15*(2), 221–232, doi:10.1175/1520-0434(2000)015¡0221:UOTORF¿2.0.CO;2.

407 Ventura, V., C. J. Paciorek, and J. S. Risbey (2004), Controlling the proportion of falsely
408 rejected hypotheses when conducting multiple tests with climatological data, *J. Climate*,
409 *17*, 4343–4356, doi:10.1175/3199.1.

410 Vose, R. S., S. Applequist, M. A. Bourassa, S. C. Pryor, R. J. Barthelmie, B. Blanton,
411 P. D. Bromirski, H. E. Brooks, A. T. DeGaetano, R. M. Dole, et al. (2014), Monitoring
412 and understanding changes in extremes: Extratropical storms, winds, and waves, *Bull.*
413 *Amer. Meteorol. Soc.*, *95*, 377–386, doi:10.1175/BAMS-D-12-00162.1.

414 Wernli, H., and C. Schwierz (2006), Surface cyclones in the ERA40 data set (1958-2001).
415 Part I: Novel identification method and global climatology, *J. Atmos. Sci.*, *63*, 2486–
416 2507, doi:10.1175/JAS3766.1.

417 Whan, K., F. Zwiers, and J. Sillmann (2016), The influence of atmospheric blocking
418 on extreme winter minimum temperatures in north america, *J. Climate*, (2016), doi:
419 10.1175/JCLI-D-15-0493.1.

Wilks, D. S. (2011), *Statistical Methods in the Atmospheric Sciences*, *International Geophysics Series*, vol. 100, 3 ed., Elsevier Inc, doi:10.1016/B978-0-12-385022-5.00001-4.

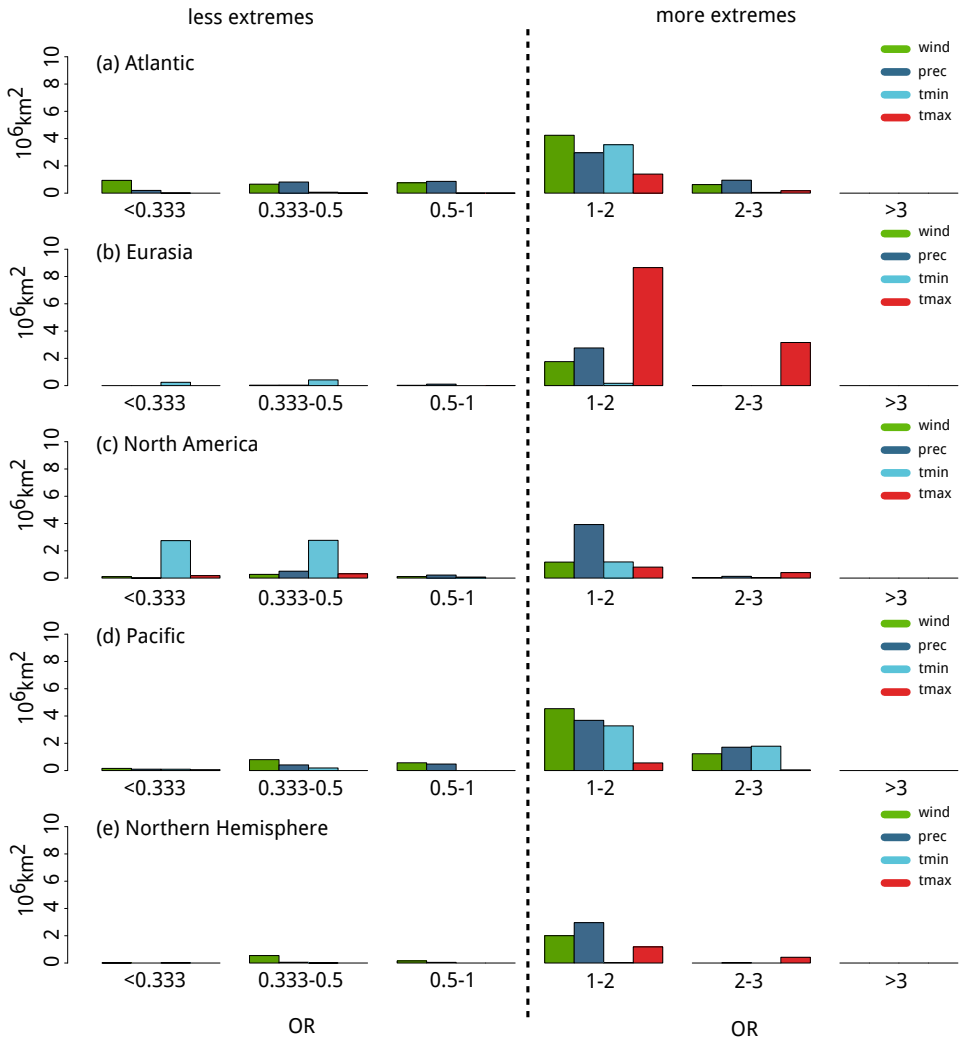

Figure 1. Land area north of 10 °N with statistically significant ORs of DJF wind (green), DJF precipitation (dark blue), DJF cold (light blue) and JJA hot (red) extremes for high waviness in the North Atlantic (a), the Eurasian (b), the North American (c) and the North Pacific (d) sector and in the entire Northern Hemisphere (e) for different OR categories.

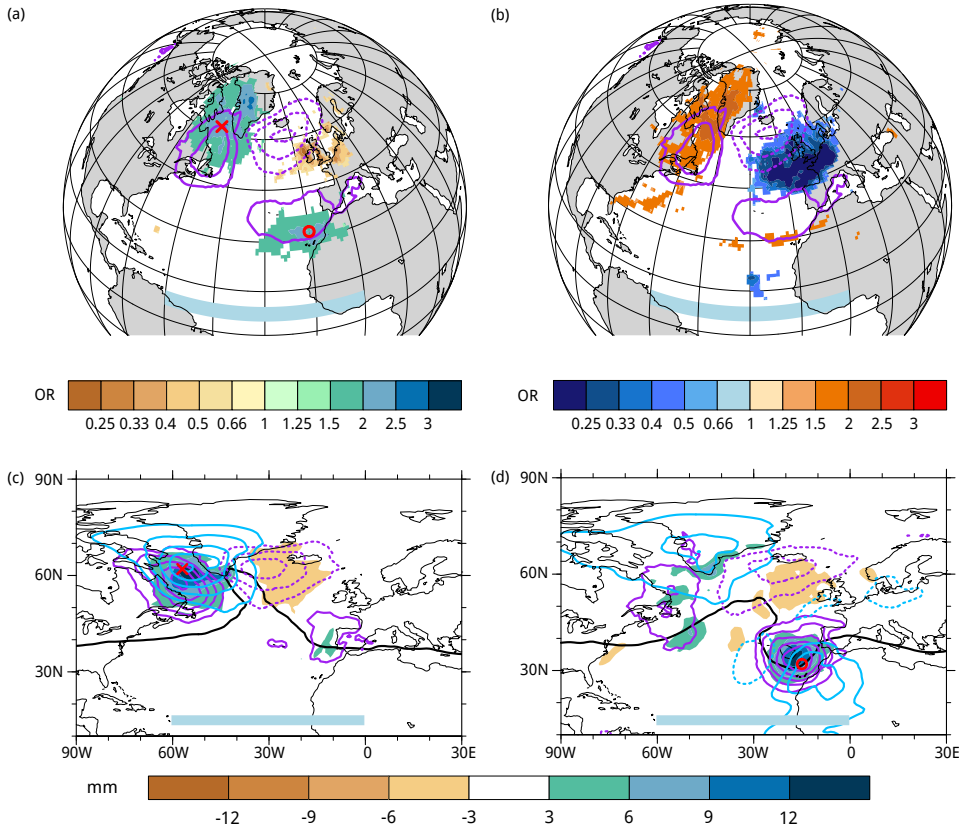

Figure 2. Statistically significant ORs of (a) precipitation and (b) wind gust extremes for high waviness in the North Atlantic sector (indicated with light blue bars). Solid (dashed) purple contours depict positive (negative) cyclone frequency anomalies for DJF high waviness days in the Atlantic sector in absolute percentage points starting from 5*pp* (-5*pp*), every 5*pp* (-5*pp*). Panels (c) and (d) depict composites of various variables for days when high waviness in the North Atlantic sector co-occurs with a precipitation extreme at 57 °W/62 °N (c) and at 15 °W/32 °N (d): Precipitation anomaly relative to the DJF daily mean precipitation (shading), cyclone frequency anomaly as in (a,b) but starting from 10pp every 10pp, composite 2 PVU contour (solid black) and standardized anomalies of the vertically integrated specific humidity in light blue, starting at plus (solid) and minus (dashed) 0.5 standard deviation, every 0.5 standard deviation. Red crosses and circles indicate the two grid points.

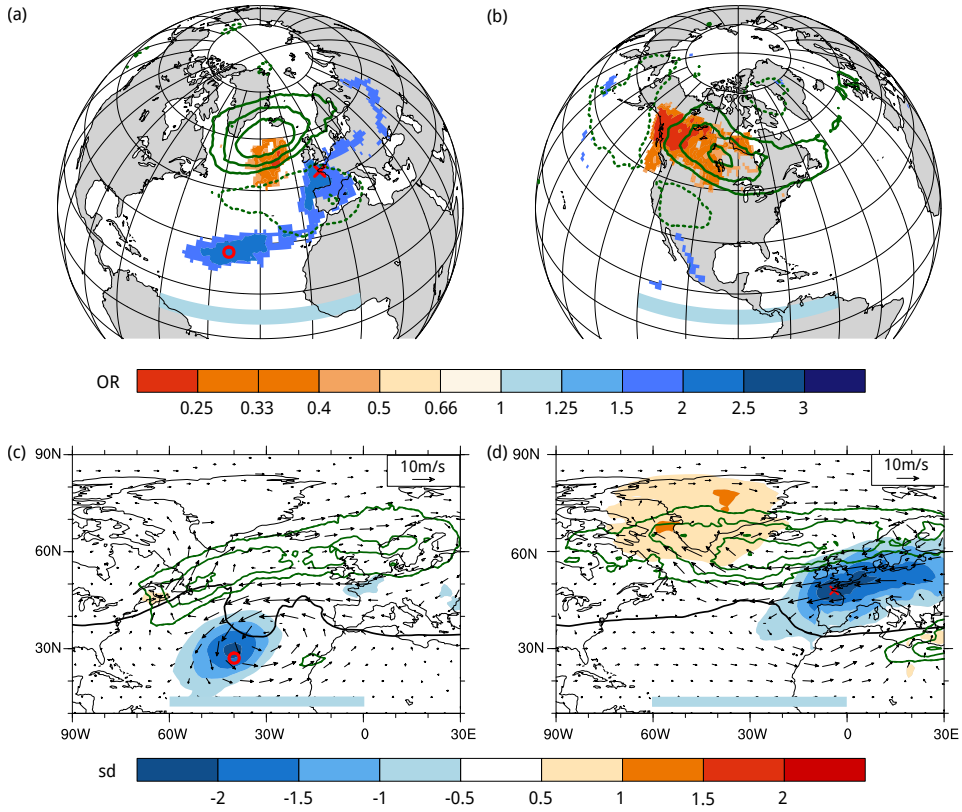

436 **Figure 3.** Statistically significant ORs of DJF cold extremes for high waviness in the (a) Atlantic and (b)
437 North American sector (sectors indicated with light blue bars in all panels). Solid (dashed) green contours
438 depict positive (negative) blocking frequency anomalies for DJF high waviness days in the respective sector in
439 absolute percentage points starting from 5*pp* (-5*pp*), every 5*pp* (-5*pp*). Panels (c) and (d) depict composites of
440 various variables for days when high waviness in the North Atlantic sector co-occurs with a precipitation ex-
441 treme at 40 °W/27 °N (c) and at 4 °W/40 °N (d): Standardized 2 m temperature anomaly (shading), blocking
442 frequency anomaly as in (a,b) but starting from 10pp every 10pp, composite 2 PVU contour (solid black) and
443 wind anomalies at 850 hPa. Red crosses and circles indicate the two grid points.

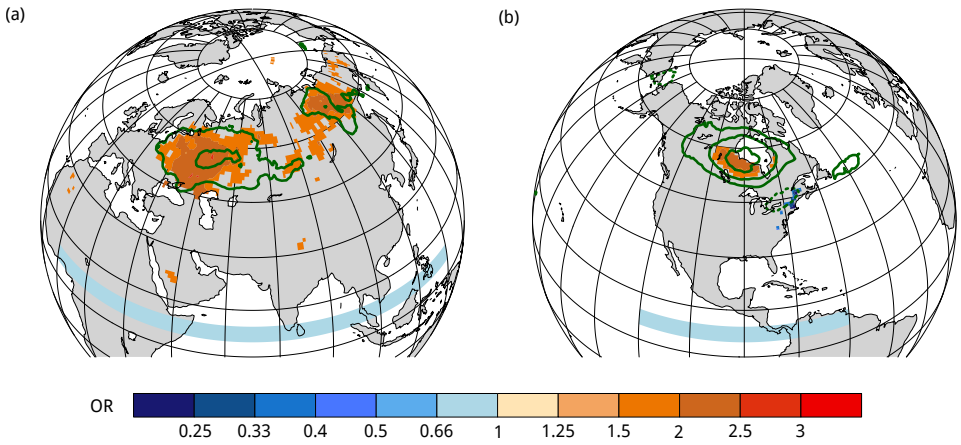

Figure 4. Statistically significant ORs of JJA hot extremes for high jet waviness in the (a) Eurasian sector and (b) the North American sector. Green contours (blocking frequency anomaly) as in Figure 3. The blue bar depicts the extent of the respective sector.